

Mechanical and dynamic mechanical properties of miscible blends of epoxidized natural rubber and poly(ethylene-*co*-acrylic acid)

Subhra Mohanty and Golok B. Nando*

Rubber Technology Centre, Indian Institute of Technology, Kharagpur 721302, India

and K. Vijayan and N. R. Neelakanthan

Department of Chemical Engineering, Indian Institute of Technology, Madras 600036, India

(Received 5 September 1995)

The mechanical and dynamic mechanical properties of blends of poly(ethylene-*co*-acrylic acid) (PEA) and epoxidized natural rubber (ENR-50) have been studied after reactive blending in various proportions in a Brabender Plasticorder. The miscibility of the blends has been studied by using a computer simulation method and experimentally confirmed by dynamic mechanical analysis. The dynamic properties of the blends exhibit single glass transition temperature (T_g) values, thus conforming to the law of miscibility. A positive deviation from the Fox equation (theoretical T_g) is a clear indication of miscibility via chemical interaction. A new β -transition peak in the blends appeared, and this is assumed to be due to the side-chain ester group vibration, confirming a chemical reaction between the *in situ* generated –OH groups of the ENR and free –COOH groups of the PEA. This leads to miscibility between the constituents forming the grafted structure, i.e. PEA-*g*-ENR. The mechanical properties exhibit a synergism above that calculated via the additivity rule. The chemical interactions have been further confirmed by swelling studies in a common solvent. Copyright © 1996 Elsevier Science Ltd.

(Keywords: miscibility; polymer blends; mechanical properties)

INTRODUCTION

A recent trend in the polymer industry is to blend two or more polymers in conventional rubber and plastic processing equipment in order to achieve a set of tailor-made properties for specific applications. Moreover, the reactive processing of polymers has now become very popular, being carried out either in an intensive mixer or in an extruder at a predetermined temperature, under specific pressure and shear conditions, for a predetermined time. The main advantage of this technique is the ease in processing, which ultimately lowers the cost and leads to savings in labour, time and energy. Quite often, this type of blending leads to new polymeric materials which have specific property advantages over those of the individual blend constituents. This type of synergism in the blend behaviour of polymers has become well established in the last two decades and has been assigned to the molecular miscibility between the blend segments or to a chemical reaction between them. This type of miscibility between the blend constituents has been variously interpreted as being due to specific interactions between the components, such as hydrogen bonding¹, dipole–dipole interactions², ion–dipole interactions³, ion–ion interactions⁴,

or repulsive interactions⁵. However, some of the blends are also reported to be miscible as a result of chemical reactions, such as transesterification reactions and the formation of covalent bonds between the blend constituents^{6,7}. In addition to these, some of the blends are found to be miscible particularly when both of the constituents are semicrystalline or crystalline in nature, as a result of iso-dimorphism or co-crystallinity^{8–10}.

Recently, Santra *et al.*^{11,12} have shown that blends of poly(ethylene-*co*-methyl acrylate) and poly(dimethylsiloxane) rubber are miscible throughout their entire composition range due to chemical reactions between the two constituents, and this miscibility has been confirmed by the occurrence of single, sharp glass transition temperatures for all of the compositions studied. These authors have also demonstrated that blends of a thermoplastic polyurethane (a polyether type) and poly(ethylene-*co*-methyl acrylate) are miscible throughout their entire composition range due to hydrogen-bond formation¹³.

Subsequently, Mohanty *et al.*¹⁴ carried out a miscibility study between blends of poly(ethylene-*co*-acrylic acid) and epoxidized natural rubber prepared by reactive processing and reported that the blends are completely miscible above 50 wt% PEA and partially miscible below 50 wt% of this component. The miscibility has been assigned as being due to chemical reactions via ester-

* To whom correspondence should be addressed

ification between the free $-\text{COOH}$ groups of the PEA and the $-\text{OH}$ groups of the ENR which are generated *in situ* during melt blending. A plausible mechanism for this reaction has been suggested by the authors in their communication¹⁴.

In this present study, we report the theoretical miscibility of blends of ENR and PEA as predicted from a computer simulation technique and confirm this miscibility from a study of both their mechanical and dynamic mechanical behaviour.

EXPERIMENTAL

Materials

Epoxidized natural rubber (ENR), containing 50 mol% of epoxy groups (Epoxyrene-50), was supplied by Messrs. Guthre, Malaysia, and had the following specifications: Specific gravity = 1.03; Mooney viscosity varying from 70–100. Poly(ethylene-*co*-acrylic acid) (PEA) (ESCOR-5001) was supplied by Exxon Chemicals Inc., Belgium, and had the following specifications: acrylic acid content = 6 wt% (2.4 mol%); melt index = 2; specific gravity = 0.93.

Preparation of the blends

Reactive blending of the components was carried out in a Brabender Plasticorder (Model PLE-330) at 150°C, using a rotor speed of 80 rpm. PEA was first melted for 2 min in the Plasticorder, and then ENR was added and blended for a further 7.5 min until a stable torque was obtained. The blends used in this work have been designated as N₀, N₃₀, N₅₀, N₇₀, and N₁₀₀, where the subscripts denote the contents (wt%) of ENR-50 in the blend.

Mechanical properties

Tensile sheets of ca. 2 mm thickness were compression moulded in a hydraulic press at 150°C under 10 MPa pressure, using a residence time of 2 min. Dumb-bell shaped specimens were punched out of the tensile sheets and subjected to tensile property measurements in a Zwick UTM (Model 1445) as per ASTM D 412. A minimum of three specimens were measured for each particular sample (blend) and the average values were reported. Tensile-set experiments after break were also performed in the Zwick UTM, with measurements being made 10 min after the break. The hardness of the samples was measured by a Shore A Durometer.

Dynamic mechanical analysis

Samples with dimensions of 10 × 5 × 0.5 mm³ were moulded in a hydraulic press and were then subjected to dynamic mechanical analysis in a Rheovibron (Model DDV-II-C) at a frequency of 11 Hz in the temperature range from –150 to +100°C.

Swelling study

A swelling study of the specimens was carried out in trichloroethylene at 70°C for different periods of time until equilibrium was attained. The initial weight and the swollen weight were measured and the percentage swelling was determined for each specimen.

RESULTS AND DISCUSSION

Theoretical prediction of miscibility

The miscibility of different homopolymer and copolymer blends through various specific interactions can be predicted theoretically with the help of a software package prepared by Graf *et al.*¹⁵. The calculations basically depend upon a knowledge of the solubility parameters, interaction parameters, molar volumes, and molecular weights for the various blend constituents. Coleman *et al.* have carried out extensive studies with different thermoplastic blend systems¹⁶. They have stated that in order to achieve molecular-level mixing of the blend constituents the value of the interaction parameter (χ) should be <0.002, which can be calculated by using the Hildebrand equation, as follows:

$$\chi = V_r/RT(\delta_A - \delta_B)^2 \quad (1)$$

where V_r is the reference volume, δ_A and δ_B are the solubility parameters of the two blend constituents, T is the temperature, and R is the molar gas constant.

The solubility parameters of the different polymers can be calculated from data published by Small¹⁷, Hoy¹⁸, and Van Kravelen¹⁹ by using the following relationship:

$$\delta = \sum f_i/V \quad (2)$$

where f_i is the molar attraction constant, and V is the molar volume.

In the present system one of the base polymers is a homopolymer, i.e. the epoxidized natural rubber, and the other component is a copolymer of ethylene and acrylic acid (6 wt%). The miscibility has been studied by using the software package with the help of molar volume, molecular weight and solubility parameter data, as given in Table 1. The solubility parameter for a random copolymer can be calculated by using the Hildebrand equation, as follows:

$$\delta = \sum \delta_i \phi_i \quad (3)$$

where δ_i and ϕ_i are the solubility parameter and volume fraction, respectively, of the homopolymers in the copolymer.

Using the data given in Table 1, the miscibility of the binary blend system has been predicted with the help of the software package. Figure 1 shows a plot of the content (wt%) of poly(ethylene-*co*-acrylic acid) in the blend as a function of the percentage of acrylic acid units in the copolymer. The immiscible region is shown in this figure by the black spotted area, with the remainder being the miscible region. As the acrylic acid content in the copolymer increases the area of the miscibility 'window' also increases, even at very low copolymer (PEA) contents in the blend compositions.

The copolymer (PEA) used in this present study

Table 1 Physical parameters of the pure constituents of the blends

Polymer	Molar volume (cm ³ mol ⁻¹)	Molecular weight (g/mole)	Solubility parameter (cal.cm ⁻³) ^{-0.5}
Epoxidized natural rubber	133.10	152.24	8.38
Polyethylene	33.00	28.06	8.00
Poly(acrylic acid)	38.00	72.06	11.92
Poly(ethylene- <i>co</i> -acrylic acid)	–	–	8.195

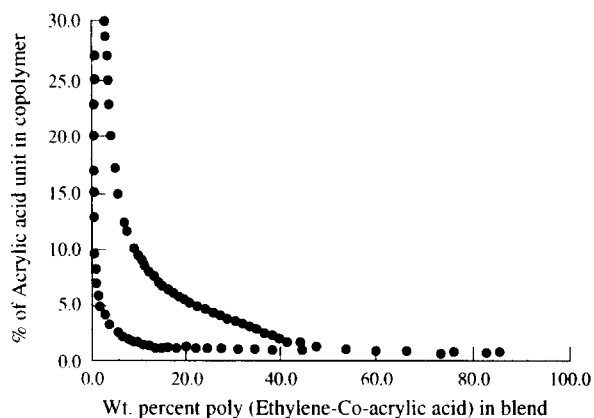


Figure 1 Miscibility 'window' plot of the content (wt%) of poly(ethylene-co-acrylic acid) in the blend vs. the percentage of acrylic acid units in the copolymer, derived from the software package of Graf et al.¹⁵

contains only 6 wt% of acrylic acid, i.e. ca. 2.4 units in a hundred units. From *Figure 1*, it is quite evident that the blend will be miscible above a level of 44 wt% PEA in the blend composition. In addition, it can be predicted that as the concentration of acrylic acid in the copolymer increases, then the blend will be miscible, even at a lower wt% of PEA. Again, by using the δ_A and δ_B values in the Hildebrand equation, with a reference volume of $100 \text{ cm}^3 \text{ mol}^{-1}$ at 25°C , the interaction parameter (χ) has been calculated and found to be 3.41×10^{-4} , which is well below the value of 0.002 predicted by the Hildebrand approach. This value substantiates the fact that the blends are completely miscible (as shown in *Figure 1*). However, when the concentration of acrylic acid in the PEA increases to 30% then the blend should be miscible throughout the composition range, i.e. from 5 to 95%, as shown in *Figure 1*.

The area below the dark circles (top line) indicate the immiscible region. Thus, if PEA contains less than 2.4% of acrylic acid units and if the proportion of PEA in the blend is less than 44 wt% then the blend will not be miscible, as shown in *Figure 1*, because of the fact that the availability of functional groups for the esterification reaction is too low for any effective compatibility to be achieved.

Mechanical properties

Table 2 shows the mechanical properties of the blends, along with those of the pure components. It is evident from *Figure 2a* that the tensile strength increases as the PEA proportion in the blend increases, starting from a very low value of 0.2 MPa for ENR (N_{100}) to 16.0 MPa for PEA (N_0). The values for the blends are intermediate to those of the pure components, but there is a synergism in all of the properties studied. This can be explained in the following way.

PEA being a copolymer of ethylene and acrylic acid, containing only 6 wt% of the latter, has a higher degree of crystallinity, due to long-range ordering in the PE segments. This is responsible for the higher strength properties of PEA and of those blends containing higher proportions of PEA. The stress-strain plots of the pure components, i.e. N_0 and N_{100} are shown in *Figure 3*. This shows that N_{100} exhibits rubbery behaviour, with no tendency for strain-induced crystallization to occur at

Table 2 Mechanical properties of the blends

Parameter	System				
	N_0	N_{30}	N_{50}	N_{70}	N_{100}
Tensile strength (MPa)	16	12.8	9.0	6.4	0.2
Elongation at break (%)	470	280	320	430	580
100% Modulus (MPa)	9.8	8.8	5.8	3.4	0.15
Set parameter (%)	350	180	120	115	30
Hardness (Shore A)	71	74	61	44	26
Degree of crystallinity (%)	42	22	15	08	00

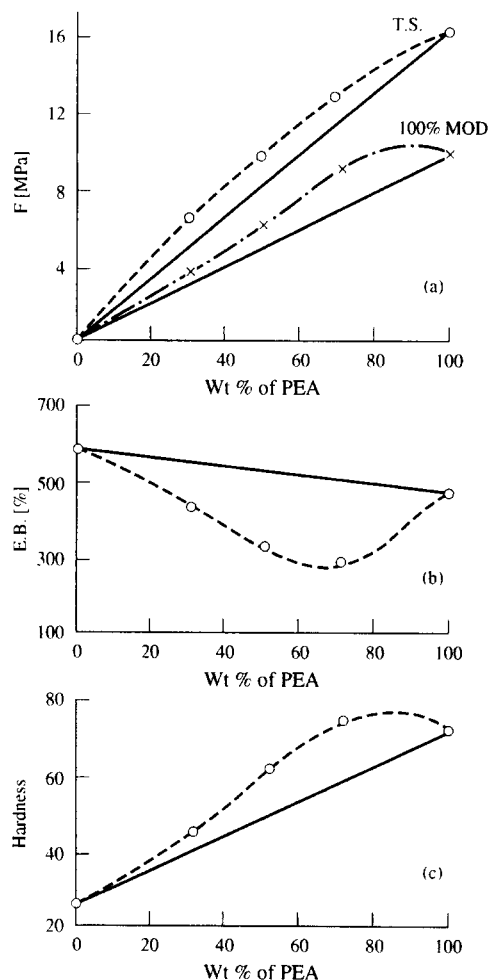


Figure 2 Mechanical properties of the blends as a function of blend composition: (a) tensile strength and 100% modulus; (b) elongation at break; (c) Shore A hardness

elongations higher than 300% due to the presence of epoxy groups in the chain which prevents any order or orientation in the chain to take place when subjected to higher strain levels. Thus, the stress value does not increase at all. The tensile strength of gum ENR is very low (0.2 MPa), even at an elongation of 560%. The stress-strain plot of N_0 shows a higher stress at lower elongation, with a yield point at ca. 20% elongation due to breakage of the crystals, beyond

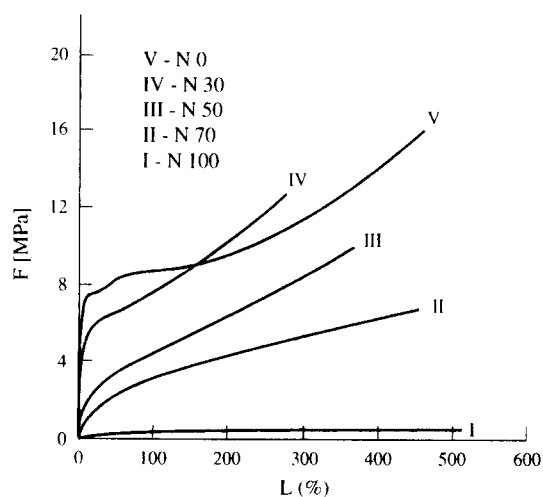


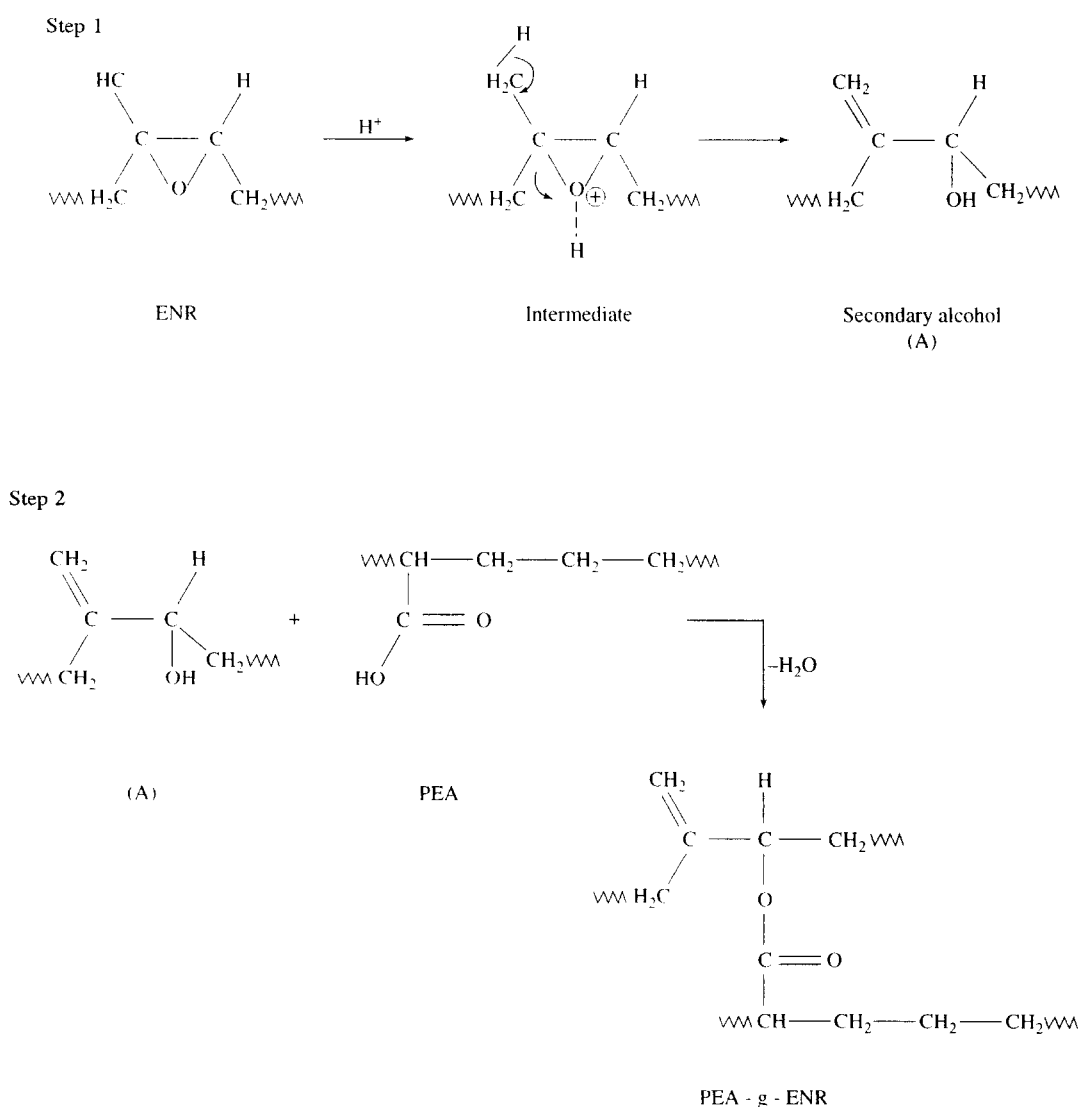
Figure 3 Stress-strain plots for five different blend compositions

which the stress value marginally increases with an increase in strain due to slippage and readjustment of the chains. Beyond 250% strain, the stress value again increases remarkably, due to ordering of the chains as a

result of strain-induced crystallization, as has been reported earlier²⁰.

Quite obviously, the blends containing a higher proportion of PEA (e.g. N₃₀) show higher tensile strengths as PEA dominates the strength property of the matrix.

The synergism in the properties may also be explained as being due to greater interactions via the chemical reactions between the blend constituents forming the grafted PEA-g-ENR structure, via the mechanism shown in Scheme 1. The formation of this structure continues to increase as the proportion of PEA in the blend increases, as predicted theoretically. Thus, the tensile strength of the blends show a positive trend, when compared to that expected from the additivity rule. This type of synergism is also observed in the case of the 100% modulus parameter. The latter increases as the proportion of PEA in the blend increases, i.e. from 0.15 to 9.8 MPa (N₁₀₀ to N₀) (Figure 2a). It is evident that below the Hookean region the increase in 100% modulus depends solely on the proportion of PEA in the blend, because beyond this region strain-induced crystallization commences, which plays a significant role. Secondly, interactions between the blend constituents through the -COOH group of the



Scheme 1

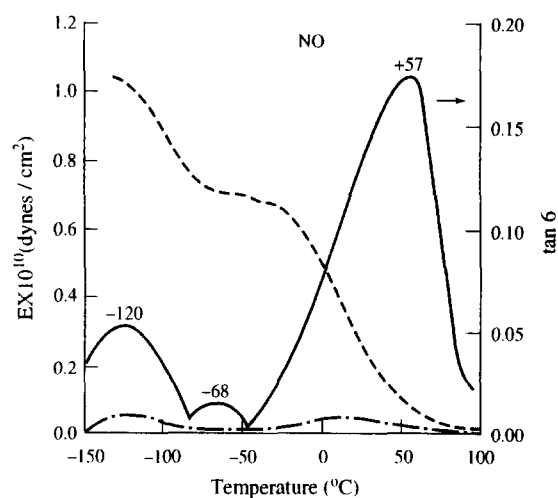


Figure 4 Dynamic mechanical properties of pure PEA (N_0) as a function of temperature: storage modulus (E'); loss modulus (E''); damping curves ($\tan \delta$)

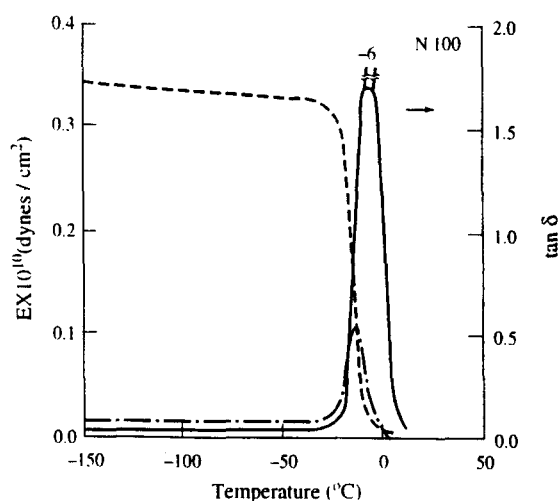


Figure 5 dynamic mechanical properties of pure ENR (N_{100}) as a function of temperature: storage modulus (E'); loss modulus (E''); damping curves ($\tan \delta$)

PEA and the $-\text{OH}$ group of the ENR (generated *in situ*) leads to esterification reactions to give the grafted structure mentioned above, thus increasing the modulus.

It is interesting to observe that the values of the elongation at break of the blends are lower than those of the pure components ENR and PEA, and that the extent of reduction is greatest in the case of the N_{30} blend (Figure 2b), as would be expected. This is obviously due to the greater interaction between the blend components (PEA and ENR) to form the familiar grafted structure, PEA-g-ENR. The proportion of the latter is increased as the proportion of PEA in the blend is increased. Since the amount of acid groups in PEA is only 6 wt% (2.4 mol%) when compared to ENR which contains 50 mol% of epoxide groups, with only a portion of these being converted into $-\text{OH}$ groups during reactive blending, an increase in the PEA concentration enhances the availability of even more $-\text{COOH}$ groups in the system, thus facilitating the formation of even more ester linkages.

The hardness measured on the Shore-A scale gradually increases as we proceed from N_{100} (26 Shore A) to N_0 (71 Shore A) (Figure 2c), whereas the hardness of the N_{30} blend is higher even than the value of 71 Shore A obtained for 100% PEA. This synergistic behaviour in the hardness of the blends is also interpreted as being due to strong interactions via the chemical reactions between the blend constituents to form the grafted structure, as explained earlier.

The tension set data measured for the pure components and the blends are shown in Table 2. The set parameter gradually decreases as the proportion of ENR in the blend increases. The sudden decrease in this parameter for N_{30} is due to both an increase in the elastic character as a result of the introduction of ENR and also to the formation of the grafted structure *in situ* during melt mixing. This has been further confirmed by a reduction in the degree of crystallinity of the blends with an increase in ENR content (Table 2). The synergistic effect in hardness, tensile strength and set properties of the blends clearly signals miscibility beyond 50 wt% of PEA, in agreement with earlier observations¹⁴. This has been further confirmed from dynamic mechanical analysis studies.

Dynamic mechanical analysis

Figure 4 shows various dynamic mechanical properties, such as storage modulus (E'), loss modulus (E'') and damping ($\tan \delta$), of the PEA copolymer with respect to variation in the temperature, ranging from -150 to 100°C . The damping curve shows three distinct transitions for the PEA copolymer, i.e. at $+57$, -68 , and -120°C , corresponding to α -, β -, and γ -relaxations, respectively. Since the melting temperature of PEA is $+98^\circ\text{C}$, the α -relaxation at 57°C , is related to the onset of molecular motion in the crystalline phase and appears as a prominent peak at this temperature. Quite often in the cases of semicrystalline and crystalline polymers this α -transition merges with the α_c transition²¹. In this case also, the α -transition appears as a shoulder and merges with the α_c -relaxation; hence it is termed as an α_c -relaxation for convenience. The β -dispersion is not very sharp, as has been observed previously in the case of the ethylene-methyl acrylate (EMA) copolymer¹¹, but appears as a hump between -45 and -75°C . This is basically due to the self-associated hydrogen bonding of the pendant acid groups. Thus, the presence of this broad hump indicates the presence of some unassociated acid groups and branching in the polyethylene backbone. The γ -relaxation occurring at -120°C is due to the small local short-range segmental motion of the 3 or 4 methylene units in a row in the amorphous region of the polyethylene chain. This is associated with the glass transition temperature of PEA, as the maximum loss (E'') also occurs near this region and the storage modulus is significantly lowered near this temperature^{22,23}. This is different from that of the long-range main-chain rotation involved in the familiar glass transition temperature of rubbers²¹. It is also observed that the storage modulus (E') is first reduced near the γ -relaxation region, and is then drastically reduced between the β - and α_c -relaxations because of the semicrystalline nature of the copolymer. The degree of crystallinity measured from wide-angle X-ray diffraction studies indicates a higher percentage crystallinity in PEA ($X_c = 42\%$).

Figure 5 shows the dynamic mechanical properties as a function of temperature for ENR-50 (N_{100}) between

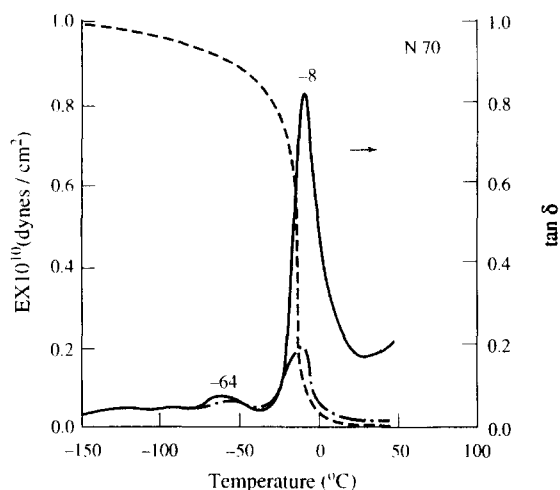


Figure 6 Dynamic mechanical properties of the N₇₀ blend as a function of temperature: storage modulus (E'); loss modulus (E''); damping curves ($\tan \delta$)

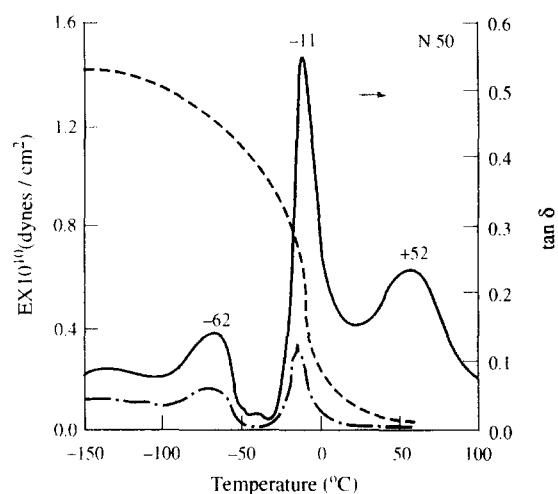


Figure 7 Dynamic mechanical properties of the N₅₀ blend as a function of temperature: storage modulus (E'); loss modulus (E''); damping curves ($\tan \delta$)

Table 3 Relaxation peaks on the damping curve ($\tan \delta$) of the blends and pure components in the temperature range from -150 to $+100^\circ\text{C}$

System	Temperature ($^\circ\text{C}$)				Theoretical T_g	E'' maximum
	α_c	α	β	γ		
N ₀	+57	-	-68	-120	-	-124
N ₃₀	+54	-14	-62	-	-18.0	-15
N ₅₀	+52	-11	-62	-	-12.0	-12
N ₇₀	-	-8	-64	-	-8.3	-11
N ₁₀₀	-	-6	-	-	-	-8

-150 and $+50^\circ\text{C}$. The storage modulus (E') of ENR-50 shows almost a plateau from -150 to -25°C , with a marginal reduction in its value, thus indicating a negligible loss of elastic character of the rubber due to the change in the average interchain spacing between entanglements on increasing the temperature. However, near the α -relaxation region, i.e. between -25 and $+5^\circ\text{C}$, E' falls drastically. The internal friction shows a maximum at -6°C , corresponding to the rubber glass transition temperature of ENR-50. The loss modulus E'' is also at a maximum near this temperature (-8°C). This is attributed to the initiation of micro-Brownian motion of the macromolecular chain segments in the molecule.

The dynamic mechanical properties of the N₇₀ blend are plotted as a function of temperature in Figure 6. It is interesting to observe that the storage modulus (E') of this blend gradually reduces from 1×10^{10} to 0.7×10^{10} dynes cm^{-2} as the temperature is raised from -150 to -25°C , while beyond this temperature there is a drastic reduction of the E' value to almost 0.01×10^{10} dynes cm^{-2} , thus signifying that the rubber glass transition temperature of the N₇₀ blend lies near to this temperature. The internal friction ($\tan \delta$) vs. temperature plot of this blend shows two distinct transitions at -8 and -64°C , corresponding to the α - and β -relaxations, respectively. The α -relaxation is basically due to the rubber glass transition temperature of the blend and is associated with the micro-Brownian motions of the molecular segments in the amorphous phase. Just below this relaxation, i.e. at -11°C , the maximum loss modulus

E'' occurs, confirming that the T_g occurs in this region. The T_g of this blend (-8°C) is found to be almost equal to that calculated from the Fox equation, i.e. -8.3°C , which confirms that the blend obeys this relationship (Table 3). The α_c -relaxation is not observed in this case, because of the smaller proportion of PEA in the blend and the predominance of the amorphous ENR which destroys the order in the crystalline zone. The degree of crystallinity is found to be only 8%. The sample becomes too soft to record any modulus in the present experimental set-up (11 Hz frequency and beyond 50°C).

Interestingly, the γ -relaxation of the N₇₀ blend completely vanishes, which may be interpreted as being due to the chemical interactions of PEA with ENR to form the grafted structure. It may also be attributed to a smaller proportion of PEA in the blend. This indicates that a glass transition temperature for PEA does not exist separately, but that the N₇₀ blend exhibits a single T_g at -8°C , which can be likened to the behaviour of a miscible blend.

It is well known that the T_g of a binary miscible blend system can be calculated theoretically by using the Fox equation²⁴ as follows:

$$\frac{W_b}{T_{gb}} = \frac{W_1}{T_{g1}} + \frac{W_2}{T_{g2}} \quad (2)$$

where W_1 , W_2 , and W_b are the contents (wt%) of component 1, component 2, and the blend (i.e. 100%), respectively, and T_{g1} , T_{g2} , and T_{gb} are the glass transition temperatures of component 1, component 2 and the blend, respectively.

The T_g value calculated for the N₇₀ blend is found to be -8.3°C , which is very close to the experimental value of -8°C . A marginally higher T_g for this blend supports the idea of an esterification reaction.

It is interesting to note that the β -transition, which is absent in the ENR, is prominently observed in this blend. This may be associated with the side-chain motion of the PEA, along with the additional ester links formed by the chemical reaction between the ENR and PEA during melt mixing, which results in a restriction of the chain mobility. Thus, the absence of both an α_c - and γ -relaxation of the PEA, along with the formation of a

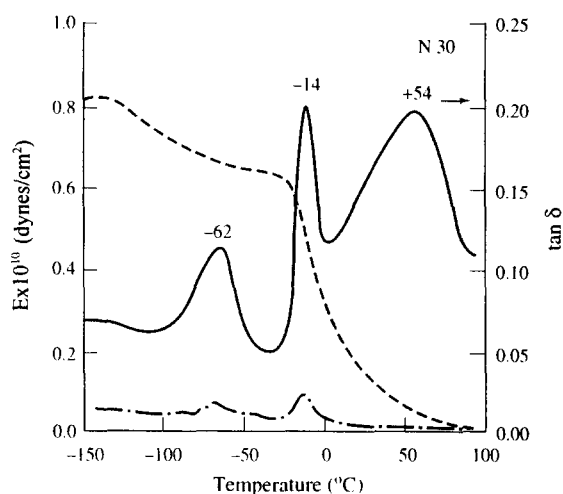


Figure 8 Dynamic mechanical properties of the N_{30} blend as a function of temperature: storage modulus (E'); loss modulus (E''); damping curves ($\tan \delta$)

single T_g at -8°C , confirms the miscibility of the N_{70} blend.

Figure 7 shows plots of loss modulus, storage modulus and internal friction ($\tan \delta$) as a function of temperature for the N_{50} blend in the temperature range from -150 to $+100^\circ\text{C}$. The E' value gradually reduces from 1.4×10^{10} , with a sharp reduction near the α -relaxation zone, signifying that the rubber glass transition occurs near this temperature. The damping curve shows three relaxations, namely α_c , α , and β , at 52 , -11 and -62°C , respectively. The α_c peak occurs at a temperature of 52°C , i.e. lower than that of the pure PEA (57°C), thus indicating that molecular motion in the crystalline phase commences at a lower temperature, while the degree of crystallinity is also reduced from 42% for N_0 to 15% for N_{50} . However, the width of the peak is increased due to an increase in the size of the crystals. The magnitude of this peak is slightly higher (0.223) than that of the pure PEA (0.175), because of the chemical reaction to form the grafted structure, with the latter also being responsible for lowering the value of the α_c -peak temperature.

The α -transition occurs at -11°C , which is slightly higher than that calculated by using the Fox equation. This is considered to represent the rubber glass transition temperature of the N_{50} blend, as the storage modulus E' reduces drastically and the loss modulus E'' shows a maximum near this temperature. According to the Fox equation, the glass transition temperature should have appeared at -12.0°C . This positive deviation from the Fox equation is again attributed to the esterification reaction between the blend components. The β -transition, which occurs at -62°C is higher than that of PEA (N_0) and is associated with the side-chain motion of the branchings in the PE moiety and the grafting of ENR through the pendent $-\text{COOH}$ groups. The increase in intensity of the β -relaxation (i.e. the magnitude), when compared to those of the N_0 and N_{70} blends, clearly indicate that the N_{50} blend has more side-chain vibrations more as a result of the highly grafted structure. The loss modulus (E'') shows a maximum just below the glass transition temperature region, i.e. at -12°C .

Figure 8 shows the plots of the dynamic mechanical

Table 4 Results obtained from swelling experiments on the blends and pure components carried out at various time intervals^a

System	Amount of swelling (%)								
	1 h	2 h	3 h	4 h	5 h	6 h	8 h	22 h	24 h
N_0	223	348	—	—	—	—	—	—	—
N_{30}	416	492	562	582	582	587	532	520	500
N_{50}	480	532	589	604	607	608	606	595	573
N_{70}	522	584	618	638	640	642	642	621	621
N_{100}	—	—	—	—	—	—	—	—	—

^a In trichloroethylene at 70°C

properties as a function of temperature for the N_{30} blend in the temperature range from -150 to $+100^\circ\text{C}$. The $\tan \delta$ curve shows three distinct relaxations at $+54$, -14 , and -62°C , corresponding, respectively, to the α_c -, α -, and β -transitions in the blend. The α_c -relaxation is related to the segmental motion in the crystalline phase, and this occurs at a slightly lower temperature than that of the PEA because of the introduction of the ENR, which disturbs the order in the crystalline phase of the PEA, reducing the degree of crystallinity to 22%. However, the magnitude of the peak is higher (0.20), due to an increase in the crystalline size. The α -relaxation occurs at -14°C , which has been interpreted as being due to the micro-Brownian motion of the main-chain segments in the blend and is attributed to the rubber glass transition temperature. On applying the Fox equation, the T_g of the blend should have appeared at -18°C , compared with the experimental value -14°C , which is well above that of the former. This type of positive deviation in the T_g value is again attributed to the transesterification reaction between the blend constituents, which results in a reduced segmental mobility¹¹. Again, the β -relaxation occurs at -62°C (cf. the N_{50} blend), which is basically due to the ester links formed in the blend and other side-chain vibrations (such as $\text{C}(1)-\text{C}(5)$) present in the polyethylene segment of the PEA. Here the peak intensity is increased due to the presence of a more highly grafted structure and the β -transition is shifted (by 6°C) towards a higher temperature because of the restriction in motion imposed by the esterification reaction.

The elastic modulus (E') decreases slowly up to a temperature of -25°C , and then falls drastically near the T_g region, i.e. the α -transition zone.

Swelling studies

Percentage swelling measurements for the blends and the pure components at different time intervals have been carried out at 70°C , and reported in Table 4. The amount of swelling is calculated by using the following:

$$\% \text{ swell} = \frac{\text{swollen wt} - \text{original wt}}{\text{original wt}} \times 100\% \quad (3)$$

Epoxidized natural rubber (ENR) (N_{100}) is completely soluble in the trichloroethylene at 70°C , while PEA (N_0) is also soluble at 70°C in the same solvent after 2 h. However, the N_{70} , N_{50} and N_{30} blends are found to be insoluble in this solvent, even after 24 h of treatment at 70°C . However, equilibrium swelling of the blends was observed after 4 h of treatment in all cases. As the percentage content of PEA is increased in the blend the

amount of swelling is decreased, which gives evidence that the addition of further PEA to the blend increases the availability of more acid units for the esterification reaction, thus resulting in a more highly grafted structure. This supports our earlier hypothesis that the extent of this reaction is at a maximum in the case of the N₃₀ blend, when compared to the N₅₀ and N₇₀ blends. This has been further supported by thermal and rheological studies of this blend system which have been reported elsewhere^{25,26}.

CONCLUSIONS

The following conclusions have been drawn from this present investigation:

1. Mechanical properties, such as the tensile strength, modulus at 100%, and hardness, show a synergistic behaviour, particularly for higher proportions of PEA in the blends.
2. The elongation at break is at a minimum for 30 wt% ENR (N₃₀), with the set parameter being drastically reduced for this blend.
3. Dynamic mechanical analysis shows single glass transition temperatures for all of the blends, implying that the blends are miscible throughout the whole composition range.
4. The experimental T_g values are found to be higher than the theoretical ones (calculated by using the Fox equation), implying that the esterification reaction between the blend constituents enhances the T_g .
5. Swelling studies provide further evidence for the occurrence of the esterification reaction to the PEA-g-ENR grafted structure, with the latter being insoluble in trichloroethylene. The amount of swelling is at a minimum for the N₃₀ blend, which implies maximum interaction between the blend constituents in this case.

REFERENCES

1 Margaritis, A. G., Kallitsis, J. K. and Kalfoglou, N. K. *Polymer* 1989, **30**, 2253

2 Varughese, K. T., Nando, G. B., De, P. P. and De, S. K. *J. Mater. Sci.* 1988, **23**, 3894

3 Eisenberg, A. and Hara, M. *Polym. Eng. Sci.* 1984, **24**, 1306

4 Murali, R. and Eisenberg, A. *J. Polym. Sci. Polym. Phys. Edn* 1982, **20**, 191

5 Stein, D. J., Jurg, R. H., Illers, K. H. and Hendas, H. *Angew. Makromol. Chem.* 1974, **36**, 89

6 Robeson, L. M. *J. Appl. Polym. Sci.* 1985, **30**, 4081

7 Porter, R. S. and Wang, L. H. *Polymer* 1992, **33**, 2019

8 Natta, G., Allegra, G., Bassi, J. W., Carlino, C., Chiellini, C. and Montagnoli, G. *Macromolecules* 1969, **2**, 311

9 Natta, G., Allegra, G., Bassi, J. W., Sianesi, D., Caporico, G. and Torti, E. *J. Polym. Sci. Part A* 1965, **3**, 4263

10 Ree, M., Kyu, T. and Stein, R. S. *J. Polym. Sci. Polym. Phys. Edn* 1987, **25**, 105

11 Santra, R. N., Roy, S., Bhowmick, A. K. and Nando, G. B. *Polym. Eng. Sci.* 1993, **33**, 1352

12 Santra, R. N., Roy, S. and Nando, G. B. *Polym. Plast. Technol. Eng.* 1994, **33**, 33

13 Santra, R. N., Chaki, T. K., Roy, S. and Nando, G. B. *Angew. Makromol. Chem.* 1993, **213**, 7

14 Mohanty, S., Roy, S., Santra, R. N. and Nando, G. B. *J. Appl. Polym. Sci.* 1994, **58**, 1947

15 Graf, J. E., Coleman, M. M. and Painter, P. C. 'Miscibility Guide and Phase Calculator' MG and PC Software, Version 1.1, Technomic Publishing Co. Inc., Lancaster, PA, 1991

16 Coleman, M. M., Graf, J. F. and Painter, P. C. 'Specific Interactions and The Miscibility of Polymer Blends', Technomic, Lancaster, PA, 1991, Ch. 7, p. 431

17 Small, P. S. *J. Appl. Chem.* 1953, **3**, 71

18 Hoy, K. L. *J. Paint Technol.* 1970, **42**, 76

19 Van Krevelen, P. W. 'Properties of Polymers', Elsevier, Amsterdam, 1972

20 Santra, R. N., Tikku, V. K. and Nando, G. B. in 'Advances in Polymer Blends and Alloys Technology' (Ed. K. Finlayson), Vol. 5, Technomic, Lancaster, PA, 1994, p. 56

21 Murayama, T. 'Dynamic Mechanical Analysis of Polymeric Materials', Material Science Monograph 1, Elsevier, New York, 1978, Ch. 3, p. 62

22 Doak, K. W. in 'Encyclopedia of Polymer Science and Engineering' (Editor-in-chief J. I. Kroschwitz), Vol. 6, Wiley Interscience, New York, 1986, p. 411

23 Zuffly, N. L., Fancher, J. A. and Bonotto, S. in 'Encyclopedia of Polymer Science and Engineering' (Eds H. F. Mark, N. Gaylord and N. M. Bikales), Vol. 6, Wiley Interscience, Sydney, 1967, p. 296

24 Fox, T. G. *Bull. Am. Phys. Soc.* 1956, **1**, 123

25 Mohanty, S., Mukunda, P. G. and Nando, G. B. *Polym. Degrad. Stabil.* 1995, **50**, 21

26 Mohanty, S., Bhattacharya, A. K., Nando, G. B. and Gupta, B. R. *Int J. Polym. Process*, in press